Short Communication:

Design, Synthesis, *In Silico* Binding Analysis, and Anticancer Evaluation of Novel Thiazole Derivatives

Amruta Jayant Waichal* **and Moreshwar Prafulla Mahajan**

Sinhgad Technical Education Society's, Sinhgad Institute of Pharmacy, Opp. Kashibai Navale Hospital, Narhe, Pune, Maharashtra, 411041. Affiliated to Savitribai Phule Pune University, Pune, Maharashtra 411007, India

** **Corresponding author:***

tel: +91-9850422123
email: amrutawaichalkhurd@gmail.com

Received: December 11, 2025
Accepted: February 7, 2026

DOI: 10.22146/ijc.114148

Abstract: *A novel thiazole-based derivative (**C1**–**C5**) incorporating amide linkages was designed and synthesized by integrating the bioactive 3,4,5-trimethoxyphenyl and 2-aminothiazole scaffolds. The structural features of the compounds were confirmed by ^{1}H-, ^{13}C-NMR, and mass spectrometry. Computational docking studies against the CBS of tubulin revealed favorable binding affinities for **C3** and **C4**, surpassing those of the reference compound CA-4. The MTT assays were used to test how well they could fight cancer by using the MCF-7 breast cancer cell line, with tamoxifen as the standard drug. Among the synthesized molecules, **C1** and **C3** exhibited the most potent cytotoxicity, reducing cell viability to 70–40%. The SAR analysis indicated that acyl substituents, particularly NO_2 and CF_3 groups, enhance cytotoxicity. Moreover, PASS prediction analysis indicated low to moderate toxicity risks, supporting the preliminary safety assessment of these compounds. Collectively, the results indicate that the synthesized thiazole derivatives serve as promising molecular scaffolds for the design of potent tubulin polymerization inhibitors with potential anticancer applications.*

Keywords: *synthesis; characterization; anticancer; thiazole; tubulin polymerization*

■ INTRODUCTION

In the past few decades, advances in drug delivery systems and drug activation have enabled more targeted delivery of medicines, increased their effectiveness and reduced their toxicity [1]. In cancer, tumor growth occurs due to the unregulated replication of mutant cells; hence, many cancer treatments target the cell division cycle. In contrast, disrupting cell division may lead to undesirable chemotherapy-related side effects, as healthy cells also undergo division during the normal cell cycle. Consequently, cancer treatment techniques that can precisely target tumor cells are widely sought after [2-4]. Tubulin, the building block of microtubules and a key player in mitosis, is among the most widely targeted chemotherapeutic targets. Vinca alkaloids and taxanes are prevalent families of natural compounds that have been widely used as inhibitors of tubulin polymerization and depolymerization, respectively [4]. Colchicine is a newer tubulin polymerization inhibitor that works by blocking the colchicine binding site (CBS). Nonetheless, the clinical use of colchicine in cancer therapy is restricted because of its narrow therapeutic window [5-6]. To overcome clinical constraints, many initiatives have been undertaken to develop CBS inhibitors (CBSIs). Despite this, several medication candidates that were created failed because they were too toxic and resistant to multiple drugs (MDR). Thus, it is imperative to create innovative CBSIs characterized by minimal toxicity and great efficacy [7]. Additionally, cancer cells are more frequently in the cell division stage than normal cells, making them more sensitive to anti-tubulin drugs [8]. Because of this, tubulins are a good target for the design and development of new cancer-fighting drugs [9-10].

In the context of developing new anticancer drugs, this study specifically examines thiazoles as a category of bioactive heterocyclic chemicals. Heterocyclic compounds constitute an important class of bioactive molecules in medicinal chemistry, owing to their

structural diversity and ability to interact with multiple biological targets. Thiazole-containing derivatives, in particular, have attracted significant attention due to their broad spectrum of pharmacological activities, including anticancer, anti-inflammatory, and antimicrobial effects. Several clinically approved and experimental anticancer agents incorporate thiazole or related heterocyclic motifs, highlighting their relevance as privileged scaffolds in drug design [11-12].

Thiazole derivatives are a type of heterocyclic compound that is very important as anticancer drugs because they have a strong affinity for numerous biological targets implicated in cancer development, such as tiazofurin [13] and bleomycin [14]. Furthermore, extensive research initiatives have been focused on enhancing the tumor-suppressive efficacy of the 2-aminothiazole core in cancer treatments, as demonstrated by the approval of alpelisib [15] and dasatinib [16] clinical use in 2019. Several 2-amino-4-phenyl thiazole compounds have been reported. El-Abd et al. synthesized compound **a** [17], while Al-Wahaibi et al. reported compound **b** [18]. Collectively, these compounds showed potent inhibition of tubulin polymerization, impaired microtubule formation, and disrupted cell cycle progression. Combretastatin A-4 is a natural trimethoxy phenyl stilbenoid [19]. However, it focuses on tubulin at the place where colchicine binds. Combretastatin A-4 and other trimethoxy phenyl-containing analogues, including the combretoxazolone analogue, have been identified as inhibitors of tubulin polymerization [20-23].

Separately, tubulin has been extensively explored as a molecular target in cancer therapy because of its essential role in mitotic spindle formation and cell division. Numerous compounds containing the 3,4,5-trimethoxyphenyl pharmacophore—such as combretastatin A-4—have been reported to bind the colchicine-binding site of tubulin. While direct biochemical validation is required to confirm tubulin polymerization inhibition, molecular docking studies offer valuable preliminary insights into potential ligand–protein interactions and binding feasibility at this site (Fig. 1).

Based on the facts above, our goal was to combine two bioactive molecules (3,4,5-trimethoxyphenyl and 2-aminothiazole) into a single small structure that would serve as the main target scaffold for the synthesis of new thiazole derivatives that could function as effective anticancer drugs. Structural modification was achieved by introducing diverse bioactive side chains onto the main scaffold and by amide derivatization. In the present study, we report the design and synthesis of a new series

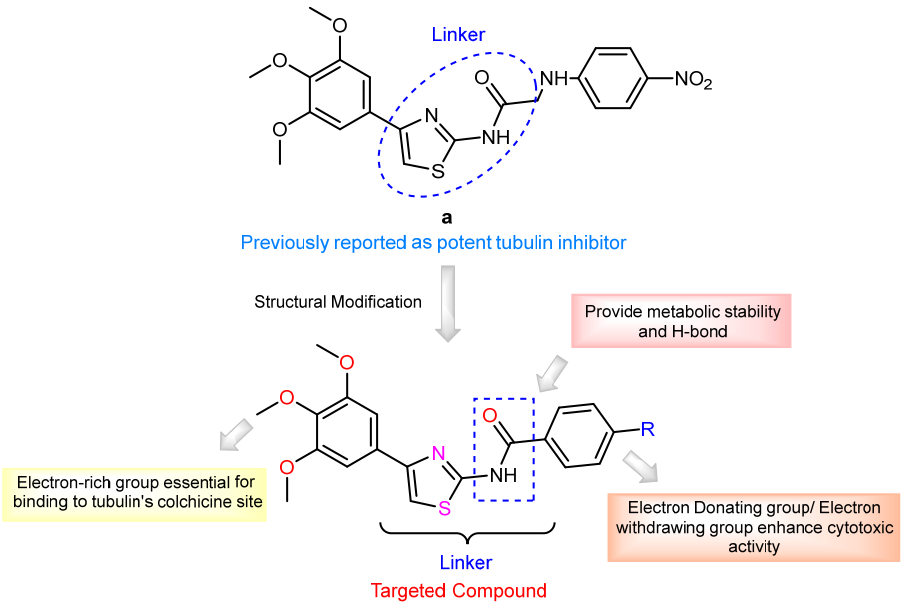

Fig 1. Rational design of a lead molecule

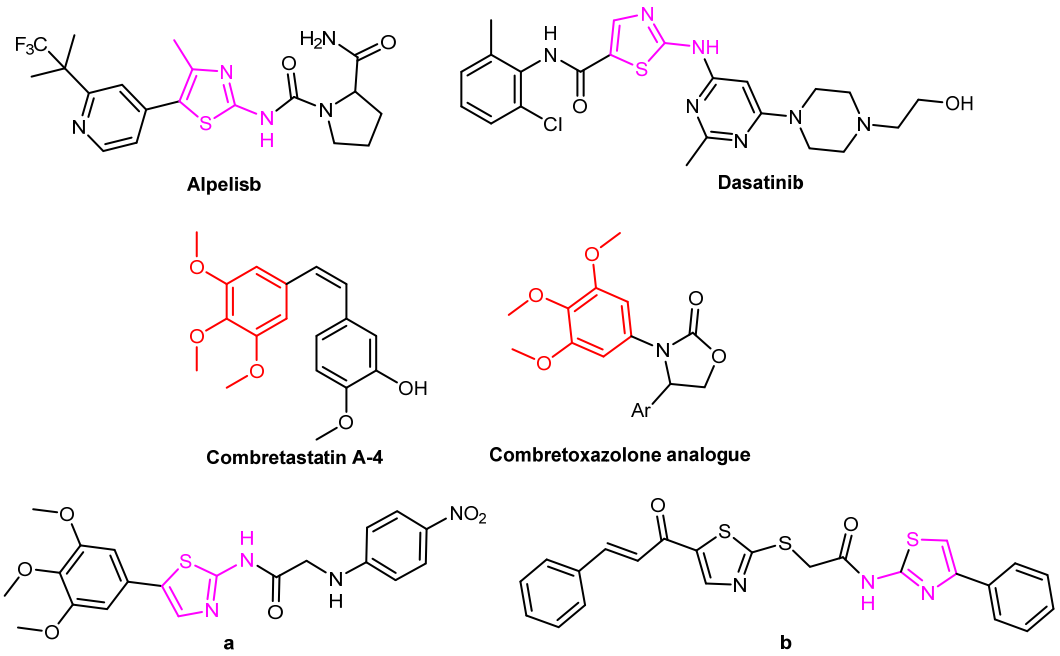

Fig 2. Chemical structure of the approved anticancer agent and reported tubulin polymerization inhibitors

of thiazole–amide derivatives incorporating the 3,4,5-trimethoxyphenyl motif. The synthesized compounds were evaluated for their antiproliferative activity against the MCF-7 breast cancer cell line using the MTT assay, with tamoxifen employed as a reference cytotoxic agent. In parallel, molecular docking studies were performed to explore the potential binding interactions of these compounds at the colchicine-binding site of tubulin. Together, these approaches aim to identify promising thiazole-based scaffolds for further optimization and mechanistic investigation as anticancer agents. The structures of the previously reported lead candidate and the recently designed scaffold are illustrated in Fig. 2.

■ EXPERIMENTAL SECTION

Materials

Required synthetic-grade reagents and chemicals were procured from reliable suppliers, i.e., 3,4,5-trimethoxyacetophenone from TCI Chemicals, cupric bromide from Loba Chemie Pvt. Ltd., thiourea from SRL, acyl chlorides from BLD Pharma, and solvents like *n*-hexane, petroleum ether, ethyl acetate, chloroform, ethanol, and dichloromethane from Thermo Fisher Scientific Pvt. Ltd.

Instrumentation

The ^{1}H and ^{13}C-NMR spectra were recorded using a Bruker Avance III HD 500 MHz instrument. Mass spectra were obtained using LC-MS on a Waters ACQUITY QDa II Mass detector; HPLC purity was determined using Shimadzu Europa GmbH; and melting points were determined using a manual Thiele tube apparatus.

Procedure

Synthetic procedure for the preparation of C1–C5

To obtain compound **C1–C5** 4-(3,4,5-trimethoxyphenyl)thiazol-2-amine (0.19 mmol) (**3**) was treated with pyridine (1.2 eq.), and after stirring in an ice bath for 5 min, the substituted acyl chloride (2–3 eq.) was added dropwise to the reaction mixture while keeping the temperature constant at 0 °C. Upon completion of the reaction, the reaction mixture was washed with cold water containing 1 M HCl and ethyl acetate, and given two washes of that and two washes of the $NaHCO_3$ solution. After that, the organic layer gets separated and subjected to column chromatography to purify the compound. The synthetic route for **C1–C5** compounds is shown in Scheme 1, and all spectroscopic data are presented in Fig. S1–S20.

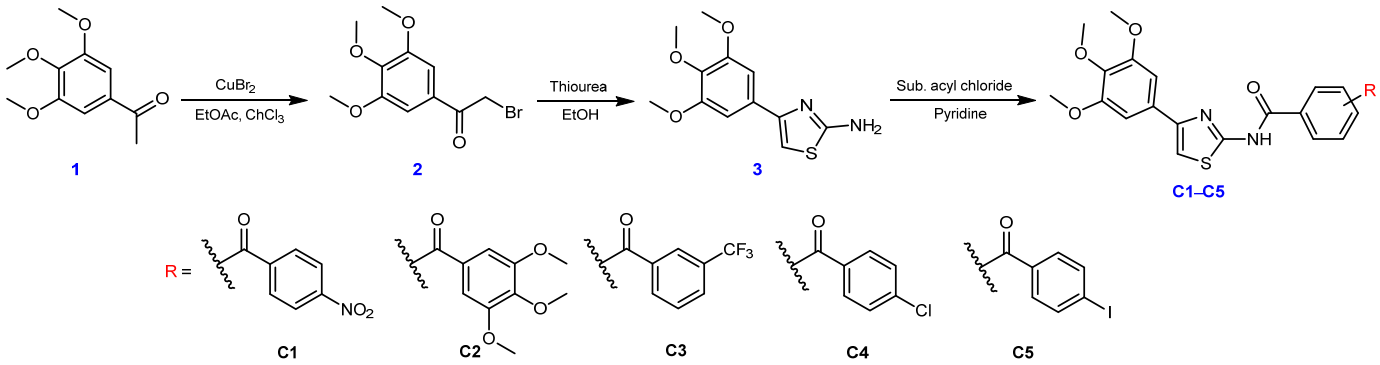

Scheme 1. The synthetic route for **C1**–**C5** compounds

4-Nitro-*N*-(5-(3,4,5-trimethoxyphenyl) thiazole-2-yl) benzamide C1. Yellow solid; yield: 28.57%; HPLC purity: 95.8%; melting point: 176–180 °C; *Rf*: 0.48 (*n*-hexane:ethyl acetate 7:3) ^{1}H-NMR (500 MHz, $CDCl_3$) δ 11.01 (*s*, 1H, NH), 8.22–8.20 (*d*, *J* = 8.8 Hz, 2H, H-25 and H-23-Ar), 8.00 (*d*, *J* = 8.8 Hz, 2H, H-26 and H-22-Ar), 7.10 (*s*, 1H, thiazole-H), 6.87 (*s*, 2H, H-2 and H-6-Ar), 3.81 (*s*, 6H, *m*-OCH_3), 3.78 (*s*, 3H, *p*-OCH_3); ^{13}C-NMR (126 MHz, $CDCl_3$) δ 163.67, 159.12, 153.35, 150.12, 137.66, 129.07, 128.67, 123.76, 108.46, 103.32, 60.74, 55.99; LC-MS: *m/z* calculated. For $C_{19}H_{17}N_3O_6S$: theoretical mass 415.42, found 414.04.

3,4,5-Trimethoxy-*N*-(5-(3,4,5-trimethoxyphenyl-thiazole2-yl) benzamide C2. Brown solid; yield: 29.03%; HPLC purity: 91.6%; melting point: 179–185 °C; *Rf*: 0.32 (*n*-hexane:ethyl acetate 7:3); ^{1}H-NMR (500 MHz, $CDCl_3$) δ 10.24 (*s*, 1H, NH), 7.22 (*s*, 2H, H-22 and H-26-Ar), 7.12 (*s*, 1H, thiazole-H), 7.02 (*s*, 2H, H-2 and H-6-Ar), 3.94 (*s*, 6H, *m*-OCH_3) 3.93 (*s*, 9H, *o,m,p*-OCH_3-Ar), 3.88 (*s*, *J* = 5.8 Hz, 3H, *p*-OCH_3); ^{13}C-NMR (126 MHz, $CDCl_3$) δ 164.51, 158.57, 153.39, 150.16, 142.15, 138.25, 133.97–130.77, 129.87, 126.83, 107.77, 104.7, 103.34, 60.94, 56.21; LC-MS: *m/z* calculated. For $C_{22}H_{24}N_2O_7S$: theoretical mass 460.13, found 460.38.

3-(Trifluromethyl)-*N*-(5-(3,4,5-trimethoxyphenyl) thiazole-2-yl) benzamide C3. White solid; yield: 30.48%; HPLC purity: 93.5%; melting point: 188–192 °C; *Rf*: 0.54 (*n*-hexane:ethyl acetate 7:3)); ^{1}H-NMR (500 MHz, $CDCl_3$) δ 11.02 (*s*, 1H, NH), 8.11 (*d*, *J* = 12.9 Hz, 2H, H-Ar), 7.78 (*d*, *J* = 7.8 Hz, 1H, H-Ar), 7.58 (*t*, *J* = 7.8 Hz, 1H, H-Ar), 7.15 (*s*, 1H, thiazole-H), 6.94 (*s*, 2H, H-2 and H-6-Ar), 3.87 (*s*, 6H, *m*-OCH_3), 3.83 (*s*, 3H, *p*-OCH_3); ^{13}C-NMR (126 MHz, $CDCl_3$) δ 163.41, 158.03, 153.40, 150.15, 138.22, 132.76, 130.70, 129.58, 124.36, 108.04, 103.38, 60.92, 56.11; LC-MS: *m/z* calculated. For $C_{20}H_{17}F_3N_2O_4S$: theoretical mass 438.09, found: 438.57.

4-Chloro-*N*-(5-(3,4,5-trimethoxyphenyl) thiazole-2-yl) benzamide C4. White solid; yield: 23.68%; HPLC purity: 92.3%; melting point: 158–164 °C; *Rf*: 0.67 (*n*-hexane:ethyl acetate 7:3); ^{1}H-NMR (500 MHz, $CDCl_3$) δ 10.09 (*s*, 1H, NH), 7.89 (*d*, *J* = 8.6 Hz, 2H, H-22 and H-26-Ar), 7.47 (*d*, *J* = 8.6 Hz, 2H, H-23 and H-25-Ar), 7.13 (*s*, 1H, thiazole-H), 7.03 (*s*, *J* = 7.3 Hz, 2H, H-2 and H-6-Ar), 3.93 (*s*, 6H, *m*-OCH_3), 3.88 (*s*, 3H, *p*-OCH_3); ^{13}C-NMR (126 MHz, $CDCl_3$) δ 170.47, 164.27, 160.28, 153.54, 148.85, 140.11, 139.59, 138.52, 131.37, 129.29, 128.93, 128.57, 107.78, 103.69, 60.94, 56.19; LC-MS: *m/z* calculated for $C_{19}H_{17}ClN_2O_4S$: 404.06, found: 405.09.

4-Iodo-*N*-(5-(3,4,5-trimethoxyphenyl) thiazole-2-yl) benzamide C5. Light brown; yield: 21.50%; HPLC purity: 91.01%; melting point: 198–205 °C; *Rf*: 0.78 (*n*-hexane:ethyl acetate 7:3); ^{1}H-NMR (500 MHz, $CDCl_3$) δ 10.46 (*s*, 1H, NH), 7.82 (*d*, *J* = 8.4 Hz, 2H, H-23 and H-25-Ar), 7.64 (*d*, *J* = 8.4 Hz, 2H, H-22 and H-26-Ar), 7.13 (*s*, 1H, thiazole-H), 7.00 (*s*, 2H, H-2 and H-6Ar), 3.92 (*s*, 6H, *p*-OCH_3), 3.87 (*s*, 3H, *m*-OCH_3); ^{13}C-NMR (126 MHz, $CDCl_3$) δ 163.67, 159.12, 153.35, 150.12, 137.66, 129.07, 128.67, 123.76, 108.46, 103.32, 60.74, 55.99; LC-MS: *m/z* calculated. For $C_{19}H_{17}IN_2O_4S$: 496.00, found: 497.00.

Biological screening

The cytotoxic potential of the synthesized compounds **C1**–**C3** was thoroughly investigated using the MTT assay, with tamoxifen serving as the standard. This colorimetric assay depends on metabolically active

cells converting MTT, a yellow tetrazolium salt, into purple formazan crystals via an enzymatic reaction. This provides a quantitative indication of the number of alive cells. The cultivated cells were evenly distributed in a 96-well plate and treated with a range of drug doses from 0.1 to 25 μM. After incubation, the formazan was dissolved, and the absorbance was calculated at 570 nm. The control wells, which were not treated, had the highest absorbance readings and were considered 100% viable [24].

Docking study

The study evaluates the binding affinity of a series of derivatives **C1**–**C5** against the receptor 4O2B. Computational docking analyses were carried out to determine the compounds' binding affinities and interaction profiles with the crystal structure of protein 4O2B, taken from the Protein Data Bank (PDB) in .pdb format. The protein molecule was optimized using BIOVIA Discovery Studio Visualizer v24.1.0.23298. The ligand molecule was drawn using ChemDraw Ultra 14.0, and the energy of the ligand was minimized using ChemDraw 3D Pro 14.0. Finally optimized for docking in AutoDock v 1.5.7 and Discovery Studio 2024 Client for interaction visualization. Combretastatin A-4 was used as the standard, and all synthesized compounds were evaluated for their potential interactions with the colchicine binding site on tubulin.

Biological activity analysis

The prediction of activity spectra (PASS) tool (https://www.way2drug.com/passonline/) was employed to estimate the potential Bioactivity profiles of the compounds. PASS analysis generates two probability values: the probability of activity (Pa) and the probability of inactivity (Pi), both ranging from 0 to 1. A higher Pa value combined with a lower Pi value indicates a greater likelihood that the predicted biological activity will be experimentally validated. In this study, the anticancer potential of tubulin polymerization inhibitor compounds was evaluated based on their Pa values. Compounds with $Pa > 0.3$ were considered to exhibit low *in silico* activity, those with $0.5 < Pa < 0.7$ were classified as having good *in silico* activity with moderate experimental relevance, and compounds with $Pa > 0.7$ were regarded as highly promising, indicating strong potential for experimental confirmation at the laboratory level [25].

■ RESULTS AND DISCUSSION

Synthesis and Purification of Compounds

Bromination of 3,4,5-trimethoxyacetophenone (**1**) with cupric bromide in ethyl acetate/chloroform promotes alpha-bromination via *in situ* generation of Br^+ and enol trapping, yielding compound 2-bromo-1-(3,4,5-trimethoxyphenyl)ethane-1-one (**2**), confirmed by ^{1}H-NMR (δ values matching literature for $–CH_2Br$ at ~4.5–5.0 ppm) [26]. Then, compound **2**, treated with thiourea in ethanol, proceeds via *S*-alkylation, followed by cyclocondensation and aromatization to 4-(3,4,5-trimethoxyphenyl)thiazol-2-amine (**3**) [22], a classic Hantzsch reaction variant. NMR confirmation aligns with reported spectra for the 3,4,5-trimethoxyphenyl-thiazole core, showing aromatic H-5 at δ 6.8–7.2 ppm and NH_2 at δ 5.0–6.0 ppm (broad). High yields reflect thiourea's bifunctionality and ethanol's role in promoting imine hydrolysis [27]. The amide-based target compounds formed by the acylation of amine **3** with substituted acyl chlorides form **C1**–**C5** via nucleophilic attack, evidenced by the downfield NH shift (δ 11.03–9.39 ppm), indicative of hydrogen-bonded amide protons. Aromatic protons (δ 6.56–8.22 ppm) as multiplets/doublets/triplets match substituted phenyl patterns, with integration confirming no side products. ^{13}C-NMR further validates: amide carbonyls (δ 165.2–162.2 ppm) and C-NH (δ 159.7–158.3 ppm) are diagnostic, shifting predictably with the electron density of acyl substituents**.** HPLC purity of compounds was carried out using an RP-C18 column (Shim-pack GIST, 250 mm × 4.6 mm, 5 μm). Mobile phase consisted of ACN:water (15:85, v/v) at a flow rate of 1.0 mL/min (pump, Shimadzu LC-20AR). The column oven (CTO-20AC) temperature was 37 °C, and the injection volume was 10 μL. The analysis was performed using a photodiode array detector (SPD-M20, Shimadzu).

In Vitro Anticancer Activity

The MTT assay results shown in Fig. 3 revealed distinct differences in the cytotoxicity of the tested compounds. Among them, Compounds **C1** and **C3** show the most pronounced cytotoxicity, decreasing viability

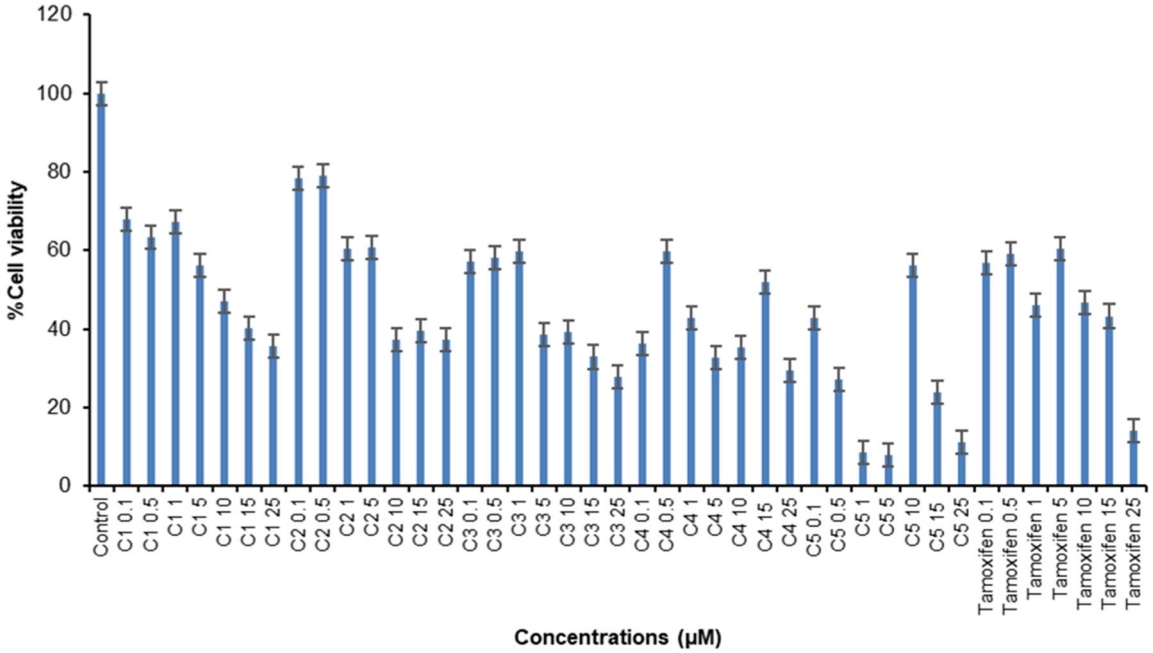

Fig 3. *In vitro* anticancer screening of the synthesized **C1**–**C5** MTT cell lines

from around 70% at 0.1 μM to below 40% at higher concentrations. Compounds **C2** exhibited inhibitory activity but were less potent, as **C2** showed gradual suppression with relatively higher viability at lower doses. Compared with tamoxifen, the reference drug, which required higher concentrations (10–25 μM) to achieve similar levels of inhibition, the synthesized compounds, particularly **C1** and **C3**, demonstrated superior potency at significantly lower doses. The MTT assay results demonstrate a clear structure-activity relationship (SAR) trend: electron-withdrawing groups enhance cytotoxicity in amide derivatives. Compounds **C1** and **C3**, bearing strong $-NO_2$ and $-CF_3$ substituents, and electron-withdrawing groups on the acyl moiety, likely stabilize the bioactive conformation through inductive withdrawal, enhancing hydrogen bonding with target proteins, such as the colchicine-binding site on tubulin. outperform tamoxifen by achieving sub-40% viability at micromolar levels far below the reference's effective range, underscoring their potential as leads for breast cancer or tubulin-targeted therapies.

Computational Study

The standard reference compound used for comparison is colchicine, which showed a docking score of (−5.6 kcal/mol). Among the tested derivatives, **C3** exhibited the strongest binding affinity (−6.3 kcal/mol), significantly surpassing colchicine. Other compounds, such as **C4** and **C5** (−6.0 and −5.9 kcal/mol, respectively), also showed better binding scores than the standard. The compounds **C1** and **C2** show the least binding affinity (−5.4 and −4.9 kcal/mol) compared to the standard Colchicine. The non-covalent interactions and binding mode of the compound against the protein are presented in Fig. 4, and the results are summarized in Table 1.

Colchicine shows a carbon-hydrogen bond with Glu207 and Glu386 to the trimethoxy group; amino acid Arg390 shows a pi-alkyl bond with the phenyl ring; and the tropylium ring shows a pi-alkyl interaction with Pro175. The compound **C3** shows amino acid interaction with Pro348, also it shows the carbon-hydrogen bond with Gln394, the methoxy group shows carbon-hydrogen bond with Ala304, the benzene ring and thio group have pi-alkyl interaction with Pro175 and Arg390, and has a binding affinity (−6.3 kcal/mol). Compound **C4** shows an amino acid interaction with Ala304 through the trimethoxy group. Chlorine group, benzene ring, and thio ring give pi-alkyl bond with Pro348, Arg390, Ala397, Met398; carboxyl group gives conventional hydrogen bond with Gln394. In compound **C5**, the trimethoxy

group shows pi-donor hydrogen bond with amino acid Pro175, Pro348, Ala397; the thio group shows pi-sigma bond with Arg390, and in the compound **C1**, it interacts with GLlu207, Ala304, and Glu386 with a trimethoxy

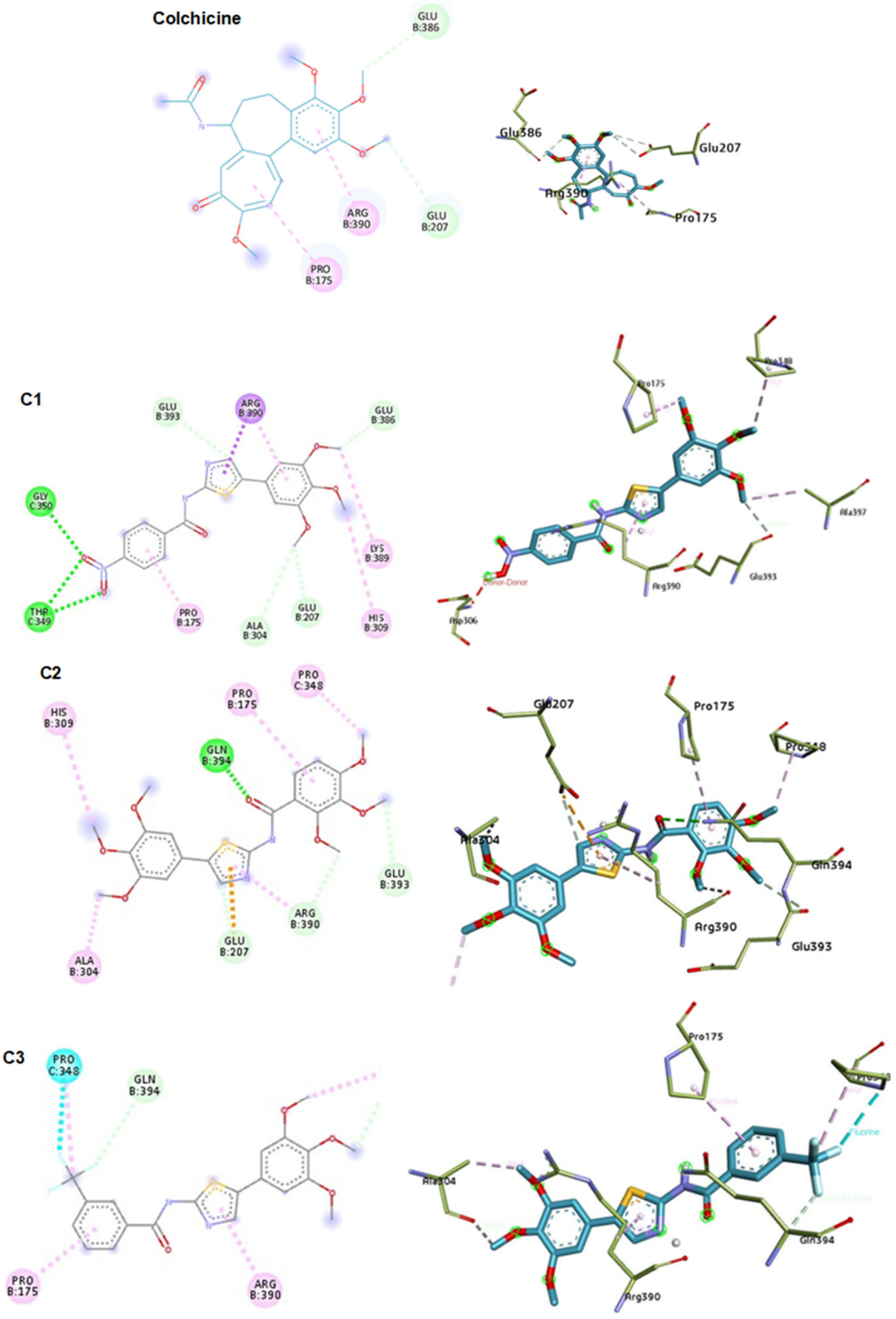

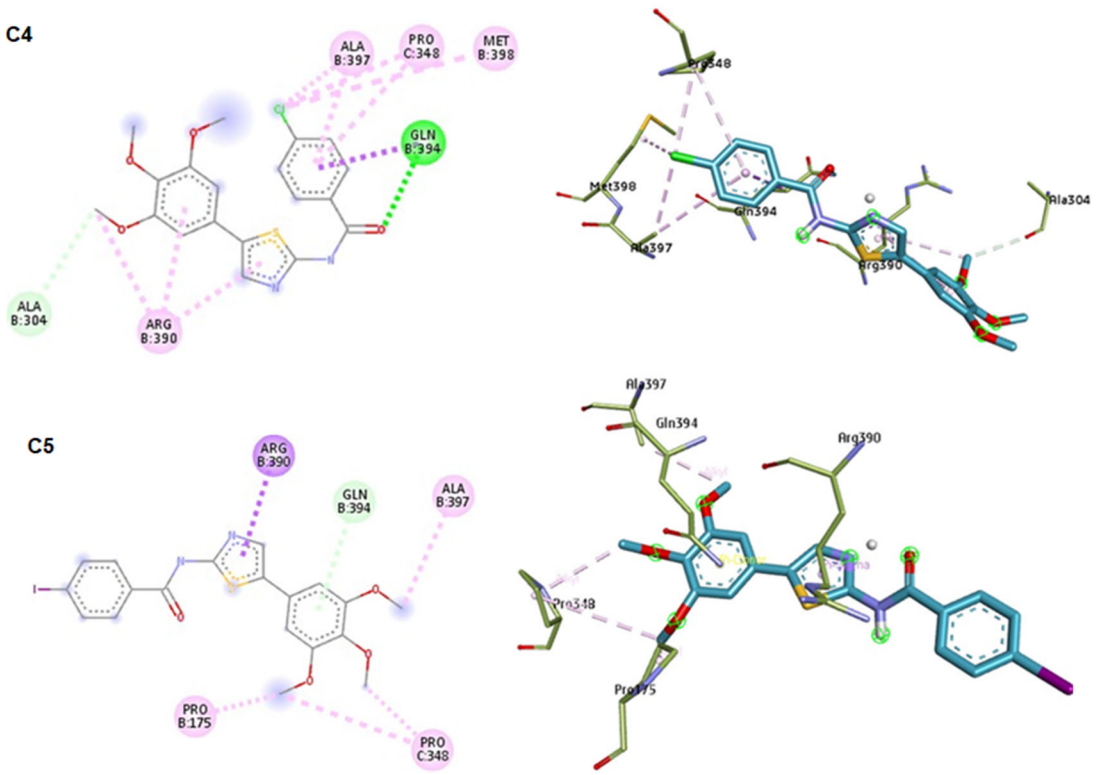

Fig 4. 2D and 3D Interactions of the compound **C1**–**C5** within the binding site of colchicine in tubulin, along with colchicine reference drug

Table 1. Docking score of the synthesized compound in the colchicine binding site

Compound	Binding energy (kcal/mol)	Type of interaction	Amino acid residues
Colchicine	−5.6	Carbon H-bond	Arg390, Pro175
		Pi-alkyl	Glu386, Glu207
C1	−5.4	Conventional H-bond	Gly350, Thr349
		Carbon H-bond	Glu393, Glu386
		Pi-sigma	Arg390
		Pi-alkyl	Lys389, His309, Pro175
C2	−4.9	Conventional H-bond	Gln394
		Carbon H-bond	Glu393, Glu207, Arg390
		Pi-alkyl	Pro175, Pro348, His309, Ala304
		Pi-anion	Glu207
C3	−6.3	Carbon H-bond	Ala304, Gln394
		Pi-alkyl	Pro175, Arg390
		Halogen (fluorine)	Pro348
C4	−6.0	Conventional H-bond	Gln394
		Carbon H-bond	Ala304
		Pi-alkyl	Arg390, Ala397, Pro348, Met398
		Pi-sigma	Gln394
C5	−5.9	Pi-donor H-bond	Gln394
		Pi-sigma	Arg390
		Alkyl	Pro175, Pro348

group, which forms a carbon-carbon hydrogen bond. Arg390 shows a pi-sigma bond with the thio ring; the nitro group over the benzene ring shows a conventional hydrogen bond with Thr349 and Gly350. The results suggest that certain thio derivatives have potential as more effective ligands for the 4O2B receptor than colchicine.

Bioactivity Analysis of the Synthesized Compound

The toxicological and mechanistic profiles of compounds **C1**–**C5** were assessed using the PASS online server, which predicts biological activities based on SAR from a large database of biologically active compounds. Predicted activities are shown as Pa (probability of activity) and Pi (probability of inactivity), both ranging from 0 to 1.000. Generally, activities with Pa higher than Pi are considered more likely to be observed experimentally. The PASS prediction Table 2 categorizes these activities into four main toxicological endpoints: mutagenicity, carcinogenicity, teratogenicity, and embryotoxicity, with representative mechanisms listed under each. Most compounds have Pa values mostly between 0.06 and 0.35, indicating plausible but not strongly pronounced activities. Regarding mutagenicity, **C1**, **C2**, **C4**, and **C5** exhibit low but detectable probabilities of inhibiting DNA helicase (Pa ≈0.064–0.081), suggesting possible interactions with DNA replication. Moderate probabilities of RNA-directed RNA polymerase inhibition are observed in **C1**, **C2**, and **C4** (Pa ≈0.257–0.262). In contrast, shikimate kinase and glycine-tRNA ligase inhibition are either absent or occur infrequently, suggesting limited mutagenic potential via these pathways. Predictions for carcinogenicity show consistently low-to-moderate Pa values for inhibition of histone deacetylase (HDAC), Bcr-Abl kinase, CDK2/cyclin A, and tyrosine kinase across the compounds. Notably, **C3** has a relatively higher probability for Bcr-Abl kinase inhibition (Pa ≈0.321), while others mostly have Pa below 0.25. These findings imply a possible role in cell-cycle control and epigenetic regulation, processes often linked to carcinogenicity and cancer treatment, although predicted levels are modest. In the teratogenicity category, all compounds show moderate probabilities for microtubule formation inhibition (Pa ≈0.189–0.304) and histone acetyltransferase inhibition (Pa ≈0.153–0.267). Lower probabilities are

Table 2. *In silico* PASS results

Compound	Pharmacological activity	Activities prediction	Pa	Pi
C1	Mutagenicity	DNA helicase inhibitor	0.077	0.009
		RNA-directed RNA polymerase inhibitor	0.262	0.196
		Glycine-tRNA ligase inhibitor	0.188	0.181
	Carcinogenicity	Histone deacetylase inhibitor	0.078	0.014
		Bcr-Abl kinase inhibitor	0.190	0.020
		CDK2/cyclin A inhibitor	0.229	0.017
		Tyrosine kinase inhibitor	0.132	0.090
	Teratogenicity	Microtubule formation inhibitor	0.213	0.038
		Beta-tubulin antagonist	0.088	0.015
		Histone acetyltransferase inhibitor	0.264	0.035
		Protein synthesis stimulant	0.126	0.115
	Embryotoxicity	Apoptosis agonist	0.273	0.144
		Aldehyde dehydrogenase inhibitor	0.235	0.108
		ATPase inhibitor	0.198	0.079
		Angiogenesis inhibitor	0.239	0.104
C2	Mutagenicity	DNA helicase inhibitor	0.081	0.008
		RNA-directed RNA polymerase inhibitor	0.262	0.196
		Shikimate kinase inhibitor	0.100	0.075
		Glycine-tRNA ligase inhibitor	0.188	0.159

Compound	Pharmacological activity	Activities prediction	Pa	Pi
	Carcinogenicity	Histone deacetylase inhibitor	0.117	0.007
		Bcr-Abl kinase inhibitor	0.254	0.008
		CDK2/cyclin A inhibitor	0.188	0.029
		Tyrosine kinase inhibitor	0.174	0.065
	Teratogenicity	Microtubule formation inhibitor	0.304	0.015
		Beta-tubulin antagonist	0.119	0.012
		Histone acetyltransferase inhibitor	0.267	0.034
		Protein synthesis stimulant	0.188	0.039
	Embryotoxicity	Apoptosis agonist	0.314	0.119
		Aldehyde dehydrogenase inhibitor	0.235	0.108
		ATPase inhibitor	0.263	0.025
		Angiogenesis inhibitor	0.338	0.054
C3	Mutagenicity	DNA helicase inhibitor	0.072	0.011
		RNA-directed RNA polymerase inhibitor	0.000	0.000
		Shikimate kinase inhibitor	0.000	0.000
		Glycine-tRNA ligase inhibitor	0.000	0.000
	Carcinogenicity	Histone deacetylase inhibitor	0.090	0.011
		Bcr-Abl kinase inhibitor	0.321	0.004
		CDK2/cyclin A inhibitor	0.138	0.054
		Tyrosine kinase inhibitor	0.143	0.081
	Teratogenicity	Microtubule formation inhibitor	0.189	0.057
		Beta-tubulin antagonist	0.043	0.031
		Histone acetyltransferase inhibitor	0.179	0.087
		Protein synthesis stimulant	0.188	0.039
	Embryotoxicity	Apoptosis agonist	0.250	0.164
		Aldehyde dehydrogenase inhibitor	0.000	0.000
		ATPase inhibitor	0.190	0.088
		Angiogenesis inhibitor	0.352	0.050
C4	Mutagenicity	DNA helicase inhibitor	0.075	0.010
		RNA-directed RNA polymerase inhibitor	0.257	0.203
		Shikimate kinase inhibitor	0.000	0.000
		Glycine-tRNA ligase inhibitor	0.000	0.000
	Carcinogenicity	Histone deacetylase inhibitor	0.072	0.016
		Bcr-Abl kinase inhibitor	0.221	0.016
		CDK2 / cyclin A inhibitor	0.181	0.032
		Tyrosine kinase inhibitor	0.168	0.068
	Teratogenicity	Microtubule formation inhibitor	0.231	0.030
		Beta-tubulin antagonist	0.063	0.020
		Histone acetyltransferase inhibitor	0.220	0.052
		Protein synthesis stimulant	0.137	0.095
	Embryotoxicity	Apoptosis agonist	0.236	0.177
		Aldehyde dehydrogenase inhibitor	0.000	0.000
		ATPase inhibitor	0.260	0.026
		Angiogenesis inhibitor	0.280	0.080

Compound	Pharmacological activity	Activities prediction	Pa	Pi
C5	Mutagenicity	DNA helicase inhibitor	0.064	0.016
		RNA-directed RNA polymerase inhibitor	0.000	0.000
		Shikimate kinase inhibitor	0.000	0.000
		Glycine-tRNA ligase inhibitor	0.000	0.000
	Carcinogenicity	Histone deacetylase inhibitor	0.076	0.015
		Bcr-Abl kinase inhibitor	0.174	0.026
		CDK2 / cyclin A inhibitor	0.000	0.000
		Tyrosine kinase inhibitor	0.130	0.092
	Teratogenicity	Microtubule formation inhibitor	0.239	0.028
		Beta-tubulin antagonist	0.066	0.020
		Histone acetyltransferase inhibitor	0.153	0.131
		Protein synthesis stimulant	0.137	0.095
	Embryotoxicity	Apoptosis agonist	0.299	0.106
		Aldehyde dehydrogenase inhibitor	0.000	0.000
		ATPase inhibitor	0.327	0.009
		Angiogenesis inhibitor	0.235	0.106

observed for beta-tubulin antagonism and protein synthesis stimulation, indicating that effects on the cytoskeleton and epigenetic regulation may be the primary developmental risks. Embryotoxicity predictions reveal relatively higher Pa values, especially for apoptosis activation, ATPase inhibition, and angiogenesis inhibition. **C2** shows the highest probability for angiogenesis inhibition (Pa ≈0.338), while **C4** and **C5** also have notable Pa values for ATPase inhibition (0.260 and 0.327, respectively). These mechanisms are key for embryonic development and energy metabolism, suggesting that any embryotoxic effects could arise from altered cell death signaling, vascular growth, or energy balance.

Overall, the PASS prediction results indicate that compounds **C1**–**C5** have low to moderate probabilities of exhibiting toxicological activities, including mutagenicity, carcinogenicity, teratogenicity, and embryotoxicity. The absence of high Pa values (> 0.7) suggests that strong toxic liabilities are unlikely, while the observed moderate probabilities highlight mechanistic pathways warranting further experimental validation.

■ CONCLUSION

In summary, a novel series of thiazole–amide derivatives incorporating a 3,4,5-trimethoxyphenyl scaffold was successfully designed, synthesized, and structurally characterized. The synthesized compounds demonstrated notable antiproliferative activity against the MCF-7 cancer cell line in the MTT assay, with **C1** and **C3** showing the most pronounced cytotoxicity at micromolar concentrations. Molecular docking studies indicated favorable binding orientations and interaction profiles of selected compounds within the colchicine-binding site of tubulin, suggesting a potential association with tubulin-related pathways. However, these findings are exploratory in nature and do not constitute direct evidence of tubulin polymerization inhibition. Additionally, *in silico* PASS analysis suggested low to moderate toxicity risks, supporting the preliminary safety profile of the synthesized molecules. Overall, the combined synthetic, biological, and computational results identify these thiazole derivatives as promising antiproliferative scaffolds worthy of further optimization and detailed mechanistic studies, including direct biochemical and cellular assays, to elucidate their precise mode of action.

■ ACKNOWLEDGMENTS

The authors express their gratitude to the management of Sinhgad Institute of Pharmacy for their support in conducting the work.

■ CONFLICT OF INTEREST

The authors declare no conflict of interest.

■ AUTHOR CONTRIBUTIONS

Amruta Jayant Waichal conducted the experiment, docking studies, and analysis. Amruta Jayant Waichal and Moreshwar Prafulla Mahajan wrote and revised the manuscript. All authors agreed to the final version of this manuscript.

■ REFERENCES

[1] Velema, W.A., Szymanski, W., and Feringa, B.L., 2014, Photopharmacology: Beyond proof of principle, *J. Am. Chem. Soc.*, 136 (6), 2178–2191.

[2] Sheldon, J.E., Dcona, M.M., Lyons, C.E., Hackett, J.C., and Hartman, M.C.T., 2016, Photoswitchable anticancer activity via *trans–cis* isomerization of a combretastatin A-4 analog, *Org. Biomol. Chem.*, 14 (1), 40–49.

[3] Karatoprak, G.S., Küpeli Akkol, E., Genç, Y., Bardakcı, H., Yücel, C., and Sobarzo-Sánchez, E., 2020, Combretastatins: An overview of structure, probable mechanisms of action and potential applications, *Molecules*, 25 (11), 2560.

[4] Wang, X., Gigant, B., Zheng, X., and Chen, Q., 2023, Microtubule-targeting agents for cancer treatment: Seven binding sites and three strategies, *MedComm – Oncol.*, 2 (3), e46.

[5] Wang, D., Xie, Y., Yan, M., Pan, Q., Liang, Y., and Sun, X., 2019, Colchicine causes prenatal cell toxicity and increases tetraploid risk, *BMC Pharmacol. Toxicol.*, 20 (1), 66.

[6] Chen, Z.H., Xu, R.M., Zheng, G.H., Jin, Y.Z., Li, Y., Chen, X.Y., and Tian, Y.S., 2023, Development of combretastatin A-4 analogues as potential anticancer agents with improved aqueous solubility, *Molecules*, 28 (4), 1717.

[7] Tian, Z., Chu, Y., Wang, H., Zhong, L., Deng, M., and Li, W., 2018, Biological activity and interaction mechanism of the diketopiperazine derivatives as tubulin polymerization inhibitors, *RSC Adv.*, 8 (2), 1055–1064.

[8] Sigalapalli, D.K., Pooladanda, V., Singh, P., Kadagathur, M., Guggilapu, S.D., Uppu, J.L., Tangellamudi, N.D., Gangireddy, P.K., Godugu, C., and Bathini, N.B., 2019, Discovery of certain benzyl/phenethyl thiazolidinone-indole hybrids as potential anti-proliferative agents: Synthesis, molecular modeling and tubulin polymerization inhibition study, *Bioorg. Chem.*, 92, 103188.

[9] Al-Hamashi, A.A., Koranne, R., Dlamini, S., Alqahtani, A., Karaj, E., Rashid, M.S., Knoff, J.R., Dunworth, M., Pflum, M.K.H., Casero, R.A., Perera, L., Taylor, W.R., and Tillekeratne, L.M.V., 2021, A new class of cytotoxic agents targets tubulin and disrupts microtubule dynamics, *Bioorg. Chem.*, 116, 105297.

[10] Sebastian, J., and Rathinasamy, K., 2023, Microtubules and cell division: Potential pharmacological targets in cancer therapy, *Curr. Drug Targets*, 24 (11), 889–918.

[11] Gümüş, M., Yakan, M., and Koca, İ., 2019, Recent advances of thiazole hybrids in biological applications, *Future Med. Chem.*, 11 (15), 1979–1998.

[12] Chhabria, M.T., Patel, S., Modi, P., and Brahmkshatriya, P.S., 2016, Thiazole: A review on chemistry, synthesis and therapeutic importance of its derivatives, *Curr. Top. Med. Chem.*, 16 (26), 2841–2862.

[13] Franchetti, P., Cappellacci, L., Grifantini, M., Barzi, A., Nocentini, G., Yang, H., O'Connor, A., Jayaram, H.N., Carrell, C., and Goldstein, B.M., 1995, Furanfurin and thiophenfurin: Two novel tiazofurin analogs. Synthesis, structure, antitumor activity, and interactions with inosine monophosphate dehydrogenase, *J. Med. Chem.*, 38 (19), 3829–3837.

[14] Childs-Disney, J.L., Yang, X., Gibaut, Q.M.R., Tong, Y., Batey, R.T., and Disney, M.D., 2022, Targeting RNA structures with small molecules, *Nat. Rev. Drug Discovery*, 21 (10), 736–762.

[15] Juric, D., Janku, F., Rodón, J., Burris, H.A., Mayer, I.A., Schuler, M., Seggewiss-Bernhardt, R., Gil-Martin, M., Middleton, M.R., Baselga, J., Bootle, D., Demanse, D., Blumenstein, L., Schumacher, K., Huang, A., Quadt, C., and Rugo, H.S., 2019, Alpelisib plus fulvestrant in *PIK3*CA-altered and *PIK3*CA-wild-type estrogen receptor–positive

advanced breast cancer: A phase 1b clinical trial, *JAMA Oncol.*, 5 (2), e184475.

[16] Saha, S.K., Gordan, J.D., Kleinstiver, B.P., Vu, P., Najem, M.S., Yeo, J.C., Shi, L., Kato, Y., Levin, R.S., Webber, J.T., Damon, L.J., Egan, R.K., Greninger, P., McDermott, U., Garnett, M.J., Jenkins, R.L., Rieger-Christ, K.M., Sullivan, T.B., Hezel, A.F., Liss, A.S., Mizukami, Y., Goyal, L., Ferrone, C.R., Zhu, A.X., Joung, J.K., Shokat, K.M., Benes, C.H., and Bardeesy, N., 2016, Isocitrate Dehydrogenase mutations confer dasatinib hypersensitivity and SRC dependence in intrahepatic cholangiocarcinoma, *Cancer Discovery*, 6 (7), 727–739.

[17] El-Abd, A.O., Bayomi, S.M., El-Damasy, A.K., Mansour, B., Abdel-Aziz, N.I., and El-Sherbeny, M.A., 2022, Synthesis and molecular docking study of new thiazole derivatives as potential tubulin polymerization inhibitors, *ACS Omega*, 7 (37), 33599–33613.

[18] Al-Wahaibi, L.H., Elshamsy, A.M., Ali, T.F.S., Youssif, B.G.M., Bräse, S., Abdel-Aziz, M., Bräse, S., Abdel-Aziz, M., and El-Koussi, N.A., 2025, Design, synthesis, *in silico* studies, and apoptotic antiproliferative activity of novel thiazole-2-acetamide derivatives as tubulin polymerization inhibitors, *Front. Chem.*, 13, 1565699.

[19] Cirla, A., and Mann, J., 2003, Combretastatins: From natural products to drug discovery, *Nat. Prod. Rep.*, 20 (6), 558–564.

[20] Karetnikov, G.L., Vasilyeva, L.A., Babayeva, G., Pokrovsky, V.S., Skvortsov, D.A., and Bondarenko, O.B., 2024, 3,4-Diarylisoxazoles—Analogues of combretastatin A-4: Design, synthesis, and biological evaluation *in vitro* and *in vivo*, *ACS Pharmacol. Transl. Sci.*, 7 (2), 384–394.

[21] Hura, N., Sawant, A.V., Kumari, A., Guchhait, S.K., and Panda, D., 2018, Combretastatin-inspired heterocycles as antitubulin anticancer agents, *ACS Omega*, 3 (8), 9754–9769.

[22] Millet, A., Plaisant, M., Ronco, C., Cerezo, M., Abbe, P., Jaune, E., Cavazza, E., Rocchi, S., and Benhida, R., 2016, Discovery and optimization of *N*-(4-(3-aminophenyl)thiazol-2-yl)acetamide as a novel scaffold active against sensitive and resistant cancer cells, *J. Med. Chem.*, 59 (18), 8276–8292.

[23] Mani, S., Swargiary, G., and Singh, K.K., 2020, Natural agents targeting mitochondria in cancer, *Int. J. Mol. Sci.*, 21 (19), 6992.

[24] Sharma, A., Sáez-Calvo, G., Olieric, N., De Asís Balaguer, F., Barasoain, I., Lamberth, C., Díaz, J.F., and Steinmetz, M.O., 2017, Quinolin-6-yloxyacetamides are microtubule destabilizing agents that bind to the colchicine site of tubulin, *Int. J. Mol. Sci.*, 18 (7), 1336.

[25] Dascalu, D., Isvoran, A., and Ianovici, N., 2023, Predictions of the biological effects of several acyclic monoterpenes as chemical constituents of essential oils extracted from plants, *Molecules*, 28 (12), 4640.

[26] El-Damasy, A.K., Jin, H., Sabry, M.A., Kim, H.J., Alanazi, M.M., Seo, S.H., Bang, E.K., and Keum, G., 2023, Design and synthesis of new 4-(3,4,5-trimethoxyphenyl)thiazole–pyrimidine derivatives as potential antiproliferative agents, *Medicina*, 59 (6), 1076.

[27] Alizadeh, S.R., and Hashemi, S.M., 2021, Development and therapeutic potential of 2-aminothiazole derivatives in anticancer drug discovery, *Med. Chem. Res.*, 30 (4), 771–806.